Disulfide-Bond Scrambling Promotes Amorphous Aggregates in Lysozyme and Bovine Serum Albumin

ARTICLE *in* THE JOURNAL OF PHYSICAL CHEMISTRY B · FEBRUARY 2015

Impact Factor: 3.3 · DOI: 10.1021/acs.jpcb.5b00144 · Source: PubMed

3 AUTHORS, INCLUDING:

Mu Yang
Michigan Technological University
4 PUBLICATIONS **11** CITATIONS
SEE PROFILE

Colina Dutta
Michigan Technological University
3 PUBLICATIONS **29** CITATIONS
SEE PROFILE

THE JOURNAL OF PHYSICAL CHEMISTRY B

Article

pubs.acs.org/JPCB

Disulfide-Bond Scrambling Promotes Amorphous Aggregates in Lysozyme and Bovine Serum Albumin

Mu Yang, Colina Dutta, and Ashutosh Tiwari*

Department of Chemistry, Michigan Technological University, Houghton, Michigan 49931, United States

Supporting Information

ABSTRACT: Disulfide bonds are naturally formed in more than 50% of amyloidogenic proteins, but the exact role of disulfide bonds in protein aggregation is still not well-understood. The intracellular reducing agents and/or improper use of antioxidants in extracellular environment can break proteins disulfide bonds, making them unstable and prone to misfolding and aggregation. In this study, we report the effect of disulfide-reducing agent dithiothreitol (DTT) on hen egg white lysozyme (lysozyme) and bovine serum albumin (BSA) aggregation at pH 7.2 and 37 °C. BSA and lysozyme proteins treated with disulfide-reducing agents form very distinct amorphous aggregates as observed by scanning electron microscope. However, proteins with intact disulfide bonds were stable and did not aggregate over time. BSA and lysozyme aggregates show unique but measurable differences in 8-anilino-1-naphthalenesulfonic acid (ANS) and 4,4′-dianilino-1,1′-binaphthyl-5,5′-disulfonic acid (bis-ANS) fluorescence, suggesting a loose and flexible aggregate structure for lysozyme but a more compact aggregate structure for BSA. Scrambled disulfide-bonded protein aggregates were observed by nonreducing sodium dodecyl sulfate polyacrylamide gel electrophoresis (SDS-PAGE) for both proteins. Similar amorphous aggregates were also generated using a nonthiol-based reducing agent, tris(2-carboxyethyl)phosphine (TCEP), at pH 7.2 and 37 °C. In summary, formation of distinct amorphous aggregates by disulfide-reduced BSA and lysozyme suggests an alternate pathway for protein aggregation that may be relevant to several proteins.

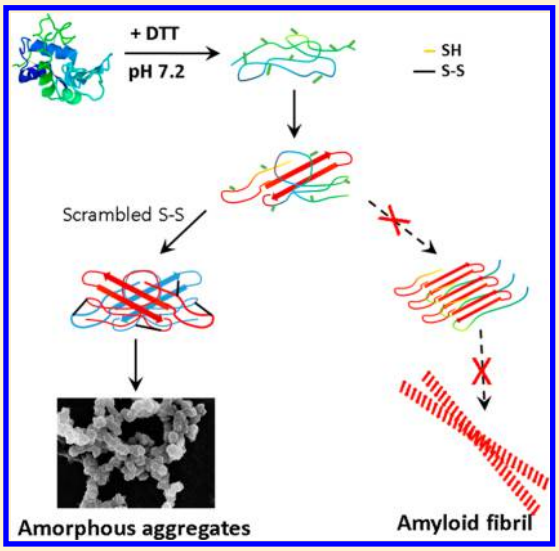

INTRODUCTION

Most proteins are functional in a narrow range of conditions where they are stable and which can be altered by changes in pH, temperature, and/or ionic strength. Once destabilized, proteins can misfold and aggregate, resulting in loss of function or a novel gain of toxic function that can lead to cellular or neuronal toxicity.[1−5] Whereas several studies have reported on the formation of amorphous or β-sheet rich amyloid-like fibrils due to denaturants and extreme pH, temperature, and/or ionic strength,[6−10] only a few studies have been carried out at or near physiological pH.[11−14] It has been suggested that most proteins can form β-sheet rich fibrils under properly designed laboratory conditions that impact inter- and intramolecular weak forces.[1,2] Interestingly, in most of the reported studies, proteins that form amyloid fibrils have intact disulfide bonds.[3,4,7,15] Disulfide bonds are critical to stabilizing protein structure and can either promote or inhibit molecular interactions affecting fibrillation,[12,16−18] leaving the relationship between disulfide bonds and protein aggregation still unclear.[19] Furthermore, previously reported studies on disulfide-reduced proteins were performed at extreme pH or temperature[16,17,20,21] in order to trigger aggregation/fibrillation. In addition, mutated or fully denatured proteins lacking disulfide bonds were found to form amyloid fibrils,[9] but these proteins are rare under physiological conditions. The cytosolic environment is highly reducing and under certain conditions may have reduced glutathione levels as high as 10 mM.[22] The cytosolic reducing agents like glutathione can break the disulfide bonds,[23] resulting in protein misfolding leading to intracellular protein aggregates or inclusions formation. On the other hand, reducing stress could also be created in extracellular environment due to excessive or improper use of antioxidants.[24−26]

In this study, we used dithiothreitol (DTT), a well-known thiol-based protein disulfide reducing agent, to investigate disulfide-bond cleavage and protein aggregation in two model proteins, hen egg white lysozyme (lysozyme) and bovine serum albumin (BSA) at pH 7.2 and 37 °C.[21,27−29] We also used a nonthiol-based reducing agent, tris(2-carboxyethyl)phosphine (TCEP), at pH 7.2 and 37 °C to verify the findings from DTT experiments. We chose lysozyme and BSA because both are globular, α-helical rich proteins containing multiple disulfide linkages.[30,31] Lysozyme is a small protein (129 amino acid

Received: January 6, 2015
Revised: February 14, 2015
Published: February 17, 2015

DOI: 10.1021/acs.jpcb.5b00144
J. Phys. Chem. B 2015, 119, 3969−3981

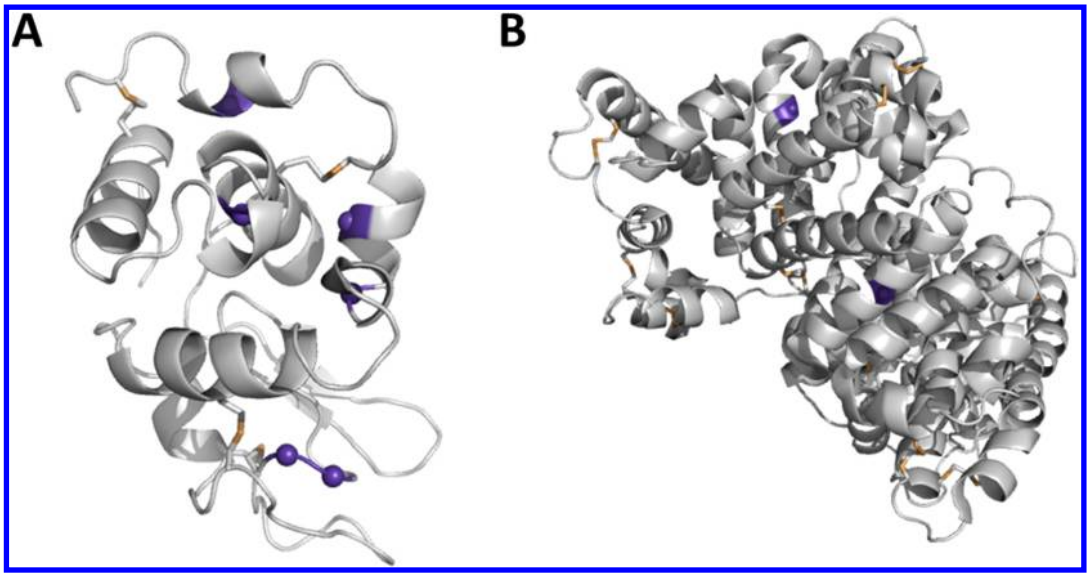

Figure 1. Structures of lysozyme (A) and BSA (B) showing the disulfide bonds (S−S, sand-yellow). The tryptophan residues are shown as purple-blue spheres. The backbone is shown in gray color. The structures were generated using PyMOL 1.3 and PDB files (1UCO)[30] for lysozyme and (4F5S)[31] for BSA.

residues; 14.3 kDa) containing 4 disulfide bridges (C6−C127, C30−C115, C64−C80, and C76−C94) and has mostly α-helices, a β-sheet, and a long loop (Figure 1). The bond C6−C127 connects N- and C-terminals of the protein and is partially exposed to solvent; the other three disulfide bonds are buried and are not solvent-accessible.[32] Lysozyme under disulfide-reducing conditions unfolds, loses its globular structure, and becomes a random coiled polypeptide.[9,33] Fibrillar, amyloid-like structures have been reported predominantly at nonphysiological pH or in the presence of denaturant such as guanidine hydrochloride.[6,9,14,34] Two other studies show that, at high temperature and neutral/near-neutral pH, lysozyme can unfold and aggregate through hydrophobic interactions, forming particulates or nonfibrillar large aggregates.[35,36] Earlier studies on lysozyme showed that, at acidic pH and high temperature, the aggregation of protein resulted in fibril formation and was dependent on disulfide-bond integrity. Fully reduced or oxidized lysozyme formed fibrils,[6,9] but the partially reduced lysozyme (50% of free −SH) did not form amyloid fibrils even after 10 days of incubation.[21] These findings are very interesting but require further study to understand the role of disulfide bonds in lysozyme aggregation.

BSA is a large protein (583 amino acid residues; ∼66 kDa) containing 17 disulfide bridges and one free cysteine and is predominantly α-helical with three homologous domains (I, II, and III) that provide a variety of binding sites on the protein (Figure 1).[31] BSA shares 76% sequence homology with human serum albumin (HSA).[8,31] Serum albumin is an abundant transport protein that binds to acidic or lipophilic ligands, such as fatty acids, bilirubin, hemin, and thyroxine, and transports them across the circulatory system.[37] At pH that is between acidic to neutral (pH 5−7), almost all the disulfide bonds are protected on BSA. However, when pH is increased from neutral to basic (pH 7−10), ∼5 disulfide bonds out of 17 become solvent-accessible and can be cleaved by a reducing agent.[38,39] In addition, raising the temperature from 35 to 55 °C also increases the number of solvent-accessible disulfide bonds on BSA.[40] Fully disulfide-reduced BSA protein was found to lose its native structure and binding abilities.[41] Although BSA is not related to any amyloidogenic disease, it is able to form aggregates that are either amorphous in nature or show amyloid fibrillar structures under certain laboratory conditions.[8,13,42,43]

Comparing and contrasting aggregation of lysozyme with BSA under identical disulfide-reducing conditions can provide insights into how disulfide bonds affect protein aggregation. Under the experimental conditions, both lysozyme and BSA formed amorphous aggregates that are significantly different from the amyloid fibrils reported in earlier studies. Interestingly, both lysozyme and BSA form amorphous aggregates that show different properties; lysozyme forms highly flexible aggregates, whereas BSA aggregates are rigid and compact.

■ MATERIALS AND METHODS

Unless otherwise indicated, all materials were used as supplied by the manufacturer without any further purification. Tris(2-carboxyethyl)phosphine (TCEP) was from Thermo Scientific Pierce; lysozyme, BSA, DTT, thioflavin T (ThT), 8-anilino-1-naphthalenesulfonic acid (ANS) dye, and 4,4′-dianilino-1,1′-binaphthyl-5,5′-disulfonic acid (bis-ANS) dye were purchased from Sigma.

Preparation of Protein Samples. Stocks of lysozyme and BSA were prepared by dissolving lyophilized protein powder in 20 mM, pH 7.2, sodium phosphate buffer having 150 mM NaCl. The protein samples reduced with TCEP were prepared in 20 mM, pH 7.2, 4-(2-hydroxyethyl)-1-piperazineethanesulfonic acid (HEPES) buffer having 150 mM NaCl instead of phosphate buffer. NaOH was added to 20 and 40 mM TCEP samples to neutralize the acidic TCEP HCl and maintain the final pH at 7.2. The protein concentrations were determined by UV−visible spectroscopy using extinction coefficient ε_{280nm} = 38 940 M^{-1} cm^{-1} and ε_{280nm} = 43 824 M^{-1} cm^{-1} for lysozyme and BSA, respectively. The working protein solutions (protein samples) had 40 μM protein in 20 mM, pH 7.2, phosphate buffer having 150 mM NaCl and 0 or 10 mM DTT. All samples were prepared on ice and then incubated at 37 °C for the indicated time periods (see figures for details). Lysozyme fibrils were prepared using the method from Krebs et al.[6] Briefly, 1

DOI: 10.1021/acs.jpcb.5b00144
J. Phys. Chem. B 2015, 119, 3969−3981

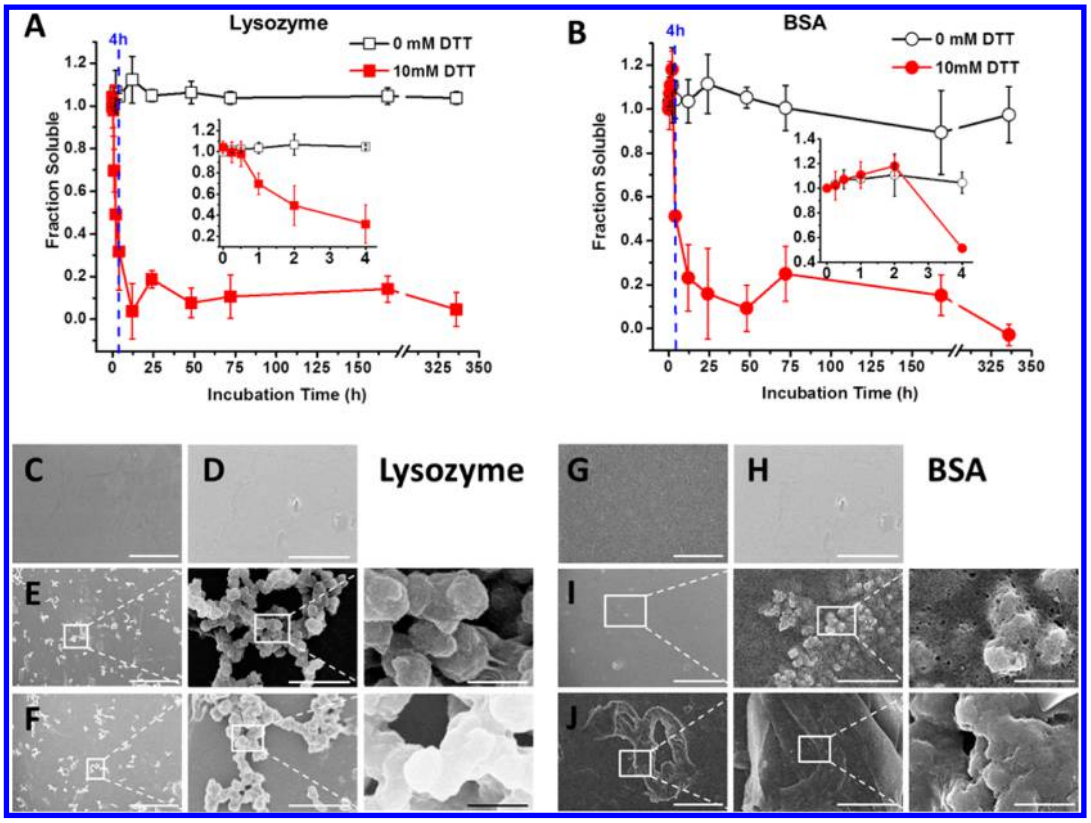

Figure 2. UV absorbance showing the fraction of soluble protein and SEM images of the insoluble aggregates. Protein samples were incubated at 37 °C for the indicated periods of time and then centrifuged. The fraction of soluble proteins in the supernatant was determined by UV absorbance at 280 nm for lysozyme (A) and BSA (B). Error bars indicate ± SD. Insoluble aggregates were imaged using SEM. The samples for lysozyme and BSA, respectively, are proteins incubated without DTT (C and G; scale bars =10 μm) and with 10 mM DTT for 0 h (D and H; scale bars =10 μm), 4 h (E and I; scale bars are 50, 5, and 1 μm from left to right), and 7 days (168 h) (F and J; scale bars are 50, 5, and 1 μm from left to right).

mM of lysozyme at pH 2.0 (in 20 mM glycine-HCl buffer) was incubated at 65 °C for 7 days to generate the fibrils.

Seeding Activity of Disulfide-Reduced Protein Aggregates. After 72 h of incubation of both lysozyme and BSA proteins with 10 mM DTT in 20 mM phosphate buffer (pH 7.2), aggregates of both proteins were washed with water and then added to 40 μM of respective protein solutions at physiological pH (20 mM phosphate buffer, pH 7.2, having 150 mM NaCl) and acidic pH (20 mM glycine-HCl buffer, pH 2.0, having 150 mM NaCl). Aggregated protein seeds were added at final concentrations of 5%, 15%, and 50% v/v, respectively. Negative controls were prepared under identical conditions but without adding seeds. All samples were prepared on ice and then incubated at 37 °C for the indicated time periods (see Figure 7 for details).

Non-Reducing Gel Electrophoresis. Incubated protein samples were mixed with 5 mM iodoacetamide (IAA) and incubated for 2 h to block any free thiol groups at room temperature. To terminate the reaction with iodoacetamide, protein samples were boiled with sodium dodecyl sulfate (SDS) sample buffer (lacking reducing agent) for 3 min. For preparing fully reduced samples, freshly prepared 40 μM protein solutions at pH 7.2 (20 mM phosphate buffer having 150 mM NaCl) were boiled with SDS sample buffer containing 10, 40, or 100 mM DTT or 5% 2-mercaptoethanol for 3 min. Lysozyme (10 μg/lane) and BSA (5 μg/lane) samples were loaded on 15% and 10% Criterion Tris-HCl polyacrylamide precast gels (Bio-Rad), respectively. Tris-glycine-SDS buffer (25 mM Tris, 192 mM glycine, 0.1% SDS, pH 8.3; Bio-Rad) was used as a running buffer, and proteins were separated by sodium dodecyl sulfate polyacrylamide gel electrophoresis (SDS-PAGE). The gels were stained with Coomassie blue stain, and the image was acquired using a scanner.

UV−Visible Absorbance Spectroscopy. All absorbance measurements were carried out on a PerkinElmer Lambda 35 UV/vis spectrometer. Protein samples were incubated for the indicated time and then centrifuged at 20 000*g* for 5 min. The supernatant was collected and diluted to 50% with 20 mM, pH 7.2, sodium phosphate buffer, and then absorbance was measured from 240 to 600 nm. All measurements were done in triplicate. Controls were similarly prepared and incubated as the samples, had all the ingredients as in the sample except protein, and were used for background subtraction.

Intrinsic and Extrinsic Fluorescence. Fluorescence measurements were performed on a Horiba Jobin Yvon spectrofluorometer (Fluoromax-4) at room temperature. The samples were diluted with phosphate buffer (20 mM, pH 7.2; for DTT-treated samples) or with HEPES buffer (20 mM, pH 7.2; for TCEP-treated samples) to a final protein concentration of 10 or 5 μM for fluorescence experiments. Intrinsic fluorescence spectra for lysozyme and BSA (5 μM) were collected in the 300−450 nm range with excitation at 280 nm. Extrinsic fluorescent dyes were dissolved in ethanol and then freshly diluted with phosphate buffer (or HEPES buffer for TCEP-treated samples) as working stocks at concentration of 350 μM (ANS), 70 μM (bis-ANS), and 700 μM (ThT) for incubation with the protein samples. Concentration of stock solutions were determined using extinction coefficients: ANS

DOI: 10.1021/acs.jpcb.5b00144
J. Phys. Chem. B 2015, 119, 3969−3981

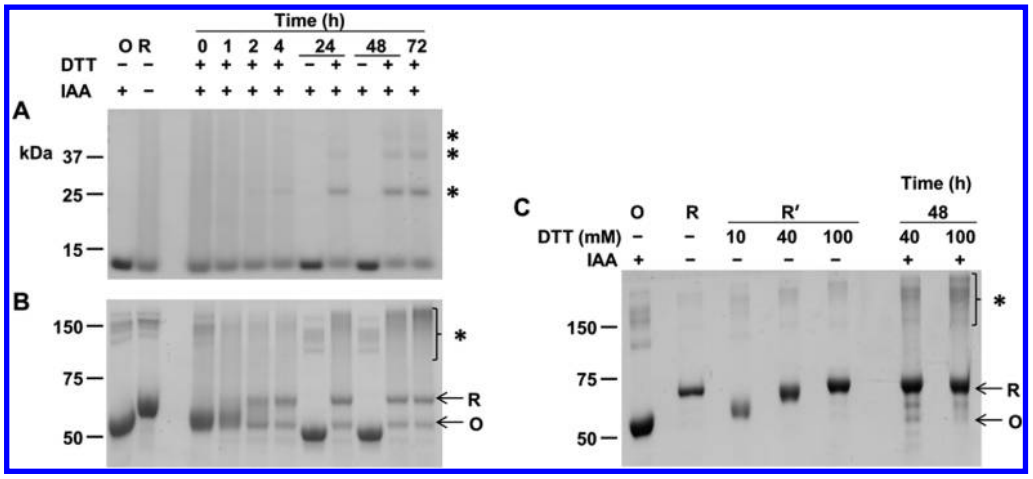

Figure 3. Nonreducing SDS-PAGE indicated the presence of high molecular weight species. Lysozyme (10 μg/lane) and BSA samples (5 μg/lane) were loaded on 15% gel (A) and 10% gel (B, C), respectively. The gels were run at 80 V for 3.5 and 4 h (lysozyme and BSA, respectively) followed by staining with Coomassie blue. Lanes "O" were fully oxidized proteins that were reacted with iodoacetamide (IAA) in the absence of DTT. Lanes "R" in panels A, B, and C were proteins that were fully reduced by 2-mercaptoethanol. Loading orders are the same for gels A and B. Lanes "R′" in panel C were BSA samples boiled in sample buffer containing 10, 40, or 100 mM DTT instead of 5% 2-mercaptoethanol. The last two lanes on panel C were BSA samples treated with 40 and 100 mM DTT for 48 h. * signifies the presence of high molecular weight protein species.

$\varepsilon_{350\ nm}$ = 5 000 M^{-1} cm^{-1}, bis-ANS $\varepsilon_{385\ nm}$ = 16 790 M^{-1} cm^{-1}, and ThT $\varepsilon_{416\ nm}$ = 26 620 M^{-1} cm^{-1}. ANS and bis-ANS were used at final concentrations of 5 and 1 μM, respectively, with 15 min equilibration with 10 μM of proteins in samples on ice. Fluorescence spectra (400−700 nm range) were collected with excitation at 380 nm for ANS and 360 nm for bis-ANS. For ThT fluorescence, 10 μM dye was incubated with 5 μM proteins on ice for 30 min, and emission spectra (460−700 nm range) were collected with excitation at 450 nm. All samples containing fluorescent dyes were incubated in the dark for the time indicated before the emission spectra were acquired. All measurements were done in triplicates. Bandwidths for excitation and emission were set at 2 nm. Controls were similarly prepared and incubated as the samples, had all the ingredients as in the sample except protein, and were used for background subtraction.

Field Emission Scanning Electron Microscopy (FESEM). All aggregate samples were analyzed on a Hitachi S-4700 FESEM, a cold field emission high-resolution scanning electron microscope. Incubated samples were aliquoted in Millipore Amicon Ultra centrifugal filters (3 kDa cutoff), and the samples were diluted with double-distilled water. The diluted samples were centrifuged and concentrated at 7 000*g* at 4 °C (three repeats after dilution with water) to wash off salts and buffer. The washed samples were aliquoted on scanning electron microscope (SEM) stubs and allowed to dry at room temperature. The samples were coated with 10 nm of platinum using a sputter coater. An acceleration voltage of 10 kV and an emission current of 5 μA were used to image the samples.

RESULTS

In this study, lysozyme and BSA proteins were incubated with 0−100 mM DTT at pH 7.2 and 37 °C for the indicated time periods, and aggregation was monitored by different techniques. Changing the concentration of DTT altered the aggregation kinetics slightly but did not affect the nature of aggregates observed (Figures S1−S4, Supporting Information). Therefore, we chose 10 mM DTT for all our subsequent studies with proteins as it showed optimum response. We incubated the proteins in the presence or absence of 10 mM DTT at pH 7.2 and 37 °C for the indicated time periods, and aggregation was monitored by different techniques. The protein samples were centrifuged; the concentration of protein in the supernatant (soluble fraction) was measured by UV−visible spectroscopy, and the morphology of the aggregates was characterized by scanning electron microscope (Figure 2). The amount of soluble protein did not change over time in the protein samples incubated in the absence of DTT (Figure 2A and B, open symbols). In addition, no aggregates were observed in the SEM images (Figure 2C and G). However, for protein samples incubated in the presence of 10 mM DTT, the fraction of soluble protein decreased significantly in 4 h (Figure 2A and B, closed symbols). After 12 h, < 20% of soluble proteins were detected in the sample solution (Figure 2A and B). Insoluble protein aggregates, as visualized by SEM, increased in amount and size as the incubation time increased for samples in the presence of 10 mM DTT (Figure 2E, F, I, and J). For both proteins, the aggregates were amorphous with an average subunit diameter of 400 ± 200 nm. Even when the DTT-treated lysozyme was incubated for a longer time (48-day sample, Figure S6, Supporting Information), the aggregates were still amorphous in nature.

Nonreducing gel electrophoresis was used to check if proteins under the experimental conditions were fully disulfide reduced or formed higher molecular weight protein species as the incubation time increased (Figure 3). For samples incubated in the absence of DTT, no new high molecular weight protein species were observed even after 48 h and the samples were comparable to freshly prepared fully oxidized protein samples (Figure 3; lane O in panels A, B, and C). Freshly prepared proteins that were fully reduced by 2-mercaptoethanol (Figure 3; lane R in panels A, B, and C) showed a slight decrease in electrophoretic mobility compared to the fully oxidized protein samples (Figure 3; lane O in panels A, B, and C) but did not show any additional higher molecular weight protein bands. While 10 mM DTT in sample buffer is not sufficient to completely reduce BSA, 40 mM and 100 mM DTT resulted in complete reduction of BSA (Figure 3; compare lanes R and R′). However, for samples incubated in the presence of 10 mM DTT, the appearance of higher

DOI: 10.1021/acs.jpcb.5b00144
J. Phys. Chem. B 2015, 119, 3969−3981

molecular weight protein species was observed for lysozyme as early as 4 h (Figure 3A). Higher molecular weight protein bands increased with increasing incubation time. In the case of BSA, the major protein band, which faded with time, is at ~66 kDa, and a smear of protein in the higher molecular weight region was observed for protein incubated for 24 h or more (Figure 3B, C). The DTT-treated BSA proteins incubated for 2 h or longer also showed a mixture of reduced (R) and oxidized (O) proteins (Figure 3B). Even BSA proteins treated with high concentrations of DTT (40 or 100 mM DTT) showed a mixture of reduced (R) and oxidized (O) proteins at 48 h (Figure 3C). To check if the high molecular weight protein species are present in the soluble fraction or not, samples from different incubation times (1, 2, 4, 24, 48, and 72 h) were centrifuged at high speed and pellets and supernatant were analyzed by nonreducing SDS-PAGE (Figure S7, Supporting Information). All high molecular weight protein species were observed in the pellet fraction only.

Conformational changes, hydrophobic exposure, and aggregation in lysozyme and BSA were monitored by intrinsic fluorescence and by extrinsic fluorophores such as 8-anilino-1-naphthalenesulfonate (ANS), 4,4′-dianilino-1,1′-binaphthyl-5,5′-disulfonic acid (bis-ANS), and Thioflavin T (ThT). Intrinsic fluorescence intensity for disulfide-reduced lysozyme increased rapidly in the first 4 h followed by a fast and significant decrease in fluorescence up to 72 h (Figure 4A).

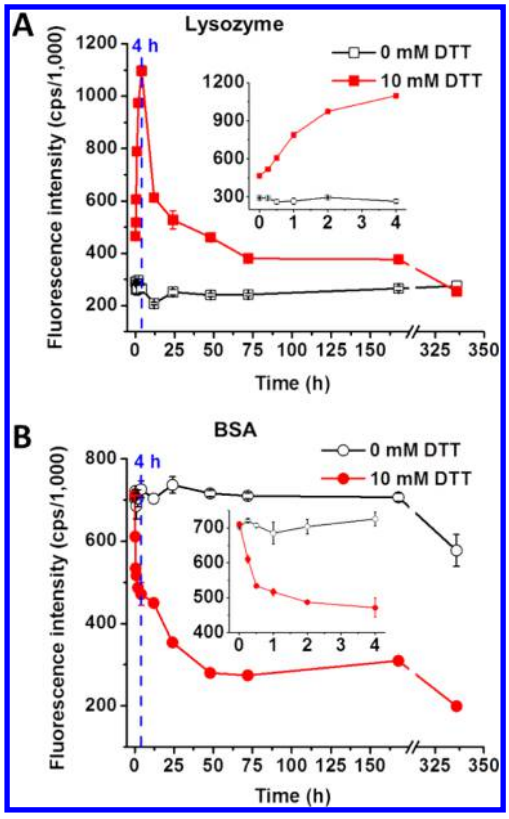

Figure 4. Intrinsic fluorescence peak intensities over time for both lysozyme and BSA proteins. Fluorescence spectra for 5 μM each of lysozyme and BSA were collected from 300 to 450 nm with excitation at 280 nm. Peak emission wavelength of 346 and 336 nm were selected for lysozyme (A) and BSA (B), respectively. Peak fluorescence intensities are shown using open symbols (without DTT) and closed symbols (with 10 mM DTT) as a function of time. Inset shows a plot for the first 4 h of incubation. Error bars indicate ± SD.

After 72 h the decrease in fluorescence intensity was slow. On the other hand, the intrinsic fluorescence for disulfide-reduced BSA showed a very rapid drop in fluorescence up to 24 h (Figure 4B). After 24 h, the decrease in fluorescence slowed down considerably. Both lysozyme and BSA that had intact disulfide bands (samples with no DTT) showed negligible fluorescence changes over time (Figure 4).

The disulfide-reduced lysozyme and BSA showed opposite trends for ANS and bis-ANS fluorescence (Figure 5). In the case of DTT-treated lysozyme samples, ANS (Figure 5A) and bis-ANS (Figure 5C) probes showed increased fluorescence with fluorescence increasing rapidly for the first 4 h (Figure 5A and C). After 4 h, the fluorescence plateaued and no significant change in fluorescence was observed as a function of time (Figure 5A and C). However, DTT-treated BSA showed a rapid decrease in ANS fluorescence for the first 4 h followed by a slower decrease in fluorescence over time (Figure 5B). Interestingly, bis-ANS showed a similar decrease in fluorescence for BSA proteins treated with or without DTT (Figure 5D). The aggregation of proteins monitored by ThT showed increased fluorescence intensity for DTT-treated lysozyme and BSA in the first 4 h (Figure 6A and B; closed symbols), whereas protein samples in the absence of DTT showed no change in ThT fluorescence (Figure 6A and B; open symbols).

SEM analysis (Figure 2) of disulfide-reduced lysozyme and BSA proteins showed that aggregates that are amorphous in nature stay amorphous even upon longer incubation. To further investigate if formation of these aggregates are seed-dependent or whether seeding can lead to fibril formation or not, we carried out cross-seeding assays at two different pHs (pH 7.2 and pH 2.0; Figure 7). The aggregates formed from 72 h incubated disulfide-reduced proteins (lysozyme and BSA) were washed and added as seeds (5%, 15%, and 50% v/v) into respective lysozyme and BSA protein solutions having intact disulfide bonds (native proteins). Proteins even with a small amount of seeds (5% v/v aggregated proteins) initiated aggregation of native proteins at pH 7.2 that share similar morphology with the seeds and showed increased binding to ThT (Figure 7A, B, E, and G). In contrast, at pH 2.0, no increase of ThT fluorescence was observed except for lysozyme and BSA, which showed an increase in ThT fluorescence with 50% seeds (Figure 7C and D). After 72 h, no structured species could be found by SEM, indicating aggregates were destabilized at acidic pH.

To further confirm the role of disulfide bonds in aggregation, we incubated protein samples with TCEP, a nonthiol-based reducing agent, and monitored protein aggregation by intrinsic and ThT fluorescence (Figure 8A–D). Because TCEP is not stable in phosphate buffer, especially around neutral pH, we changed the buffer to HEPES (20 mM, pH 7.2). Changing the buffer from phosphate (20 mM, pH 7.2) to HEPES (20 mM, pH 7.2) did not affect any measured biophysical properties of the proteins. However, the intrinsic fluorescence data for TCEP-treated lysozyme samples showed an increase in fluorescence in the first 4 h, a trend similar to DTT-treated samples, but upon longer incubation the fluorescence remained steady instead of decreasing in intensity (Figures 4A and 8A). Then, intrinsic fluorescence for TCEP-treated BSA, and ThT fluorescence for lysozyme and BSA, showed trends similar to that observed for DTT-treated protein samples (Figures 4B, 6A and B, and 8B–D). SEM images showed amorphous aggregates for proteins incubated with 2 mM TCEP (Figure 8E and F) that share morphology similar to aggregates seen for proteins

DOI: 10.1021/acs.jpcb.5b00144
J. Phys. Chem. B 2015, 119, 3969–3981

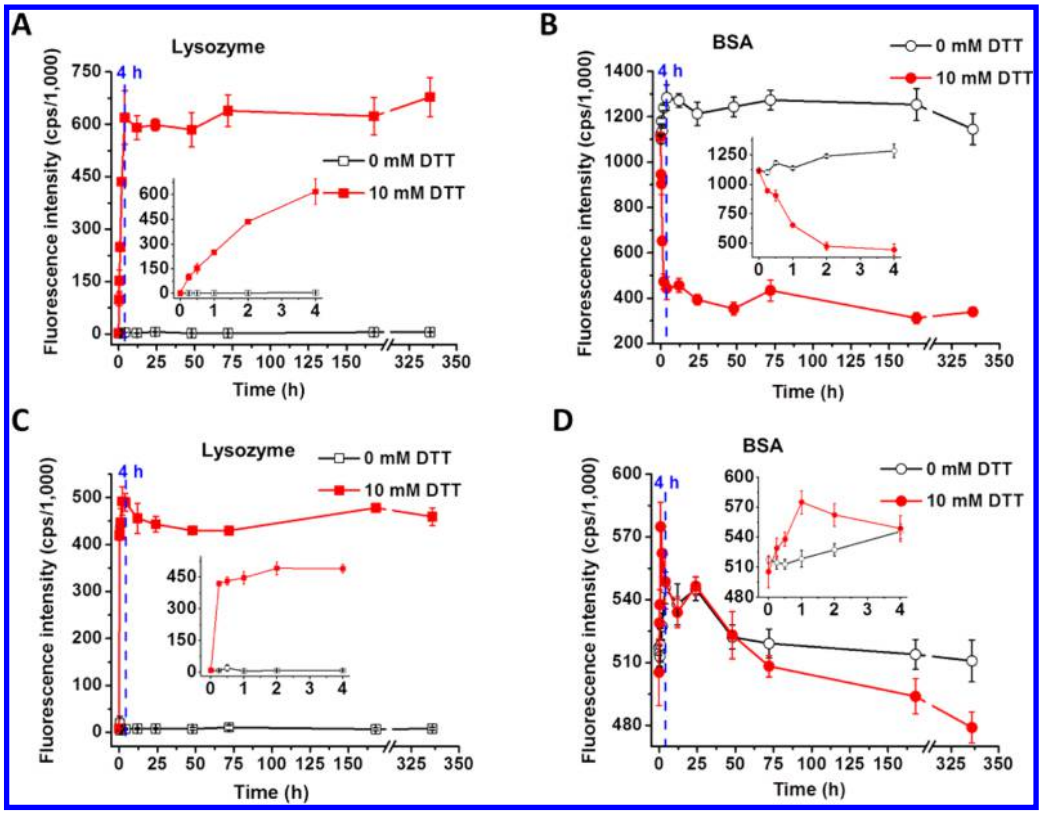

Figure 5. Changes in protein hydrophobicity and aggregation were monitored by ANS and bis-ANS fluorescence. Ten μM protein samples were incubated with 5 μM ANS or 1 μM bis-ANS for 15 min before acquiring spectra. Emission spectra for lysozyme (A and C) and BSA (B and D) were collected from 400 to 700 nm with excitation at 380 nm for ANS and 360 nm for bis-ANS. Average emission peak wavelengths of 471 and 484 nm were selected for ANS (A and B) and bis-ANS (C and D), respectively. Peak fluorescence intensities are shown using open symbols (without DTT) and closed symbols (with 10 mM DTT). The inset shows the plot for the first 4 h of incubation. Error bars indicate ± SD.

incubated with 10 mM DTT (Figure 2E, F, I, and J). Interestingly, we did not observe visible aggregates of either lysozyme or BSA incubated with 5 mM or higher TCEP in 24 h. This is similar to SEM images of lysozyme and BSA proteins in the absence of reducing agent (Figure 2C and G).

DISCUSSION

Disulfide bonds are formed naturally in 65% of secreted proteins, 15% of human proteome, and in >50% of amyloidogenic proteins.[19] The native disulfide bonds are critical for correct folding and normal function of proteins, and the disruption of disulfide bonds was shown to alter protein structures and even result in protein aggregation.[9,23,44] Although cellular redox status can be tuned by certain reducing agents,[26] cells have a great coping mechanism to resist changes. In this study we chose DTT, a disulfide-reducing agent, to mimic the excessive or improper use of thiol-based antioxidants at physiological pH and temperature. The role of disulfide bonds have been previously studied using strong reducing agents,[45] single-site mutations,[9] artificial disulfide linkages,[18] and/or at extreme pH conditions.[16] Therefore, we wanted to study how disulfide-reduced proteins misfold and form aggregates at physiological pH in the absence of any other destabilizing influences. The two proteins (lysozyme and BSA) used in this study could form amorphous aggregates but with unique structural properties.

UV absorbance and fluorescence spectroscopy data showed that both lysozyme and BSA protein samples that lack DTT were stable at 37 °C up to 2 weeks with no measurable changes in their spectral properties (Figures 2 and 4–6). In addition, no visible aggregates were observed for the proteins by SEM (Figure 2C and G). This suggests that these two proteins are stable at pH 7.2 and 37 °C for the long term in the absence of any destabilizing influence. However, for proteins incubated at 37 °C in the presence of reducing agent (10 mM DTT), we observed amorphous aggregates appearing as early as 2 h (data not shown), signifying the importance of disulfide-bond integrity in providing protein stability. This is in contrast to the fibrils found in several previous studies performed at extremes of pH or temperature in combination with other solvent additives.[9,20,23,34] The amorphous aggregates in this study are ~400 nm in diameter with a maximum length of 30 μm (Figure 2); they shares some physicochemical characteristics with protofibril, such as size (lysozyme aggregates) and ThT binding capacity. An earlier study shows that ThT positive amorphous aggregates were able to convert into protofibrils after long-term incubation and eventually formed a long, unbranched fibril structure.[46] However, under our experimental conditions, the DTT-treated aggregates were not able to convert into fibrils with increased incubation time (Figure S6, Supporting Information). Although DTT-treated lysozyme and BSA aggregates show a rapid increase in ThT fluorescence (Figure 6A and B), the ThT signal from aggregates is low and about 1/5th compared to a mature fibril under identical experimental conditions (Figure 6C). ThT is a well-known dye for characterizing amyloid-like structures;[47] however, recent studies have shown that some nonfibril/amorphous aggregates were able to bind ThT and show ThT characteristic

DOI: 10.1021/acs.jpcb.5b00144
J. Phys. Chem. B 2015, 119, 3969–3981

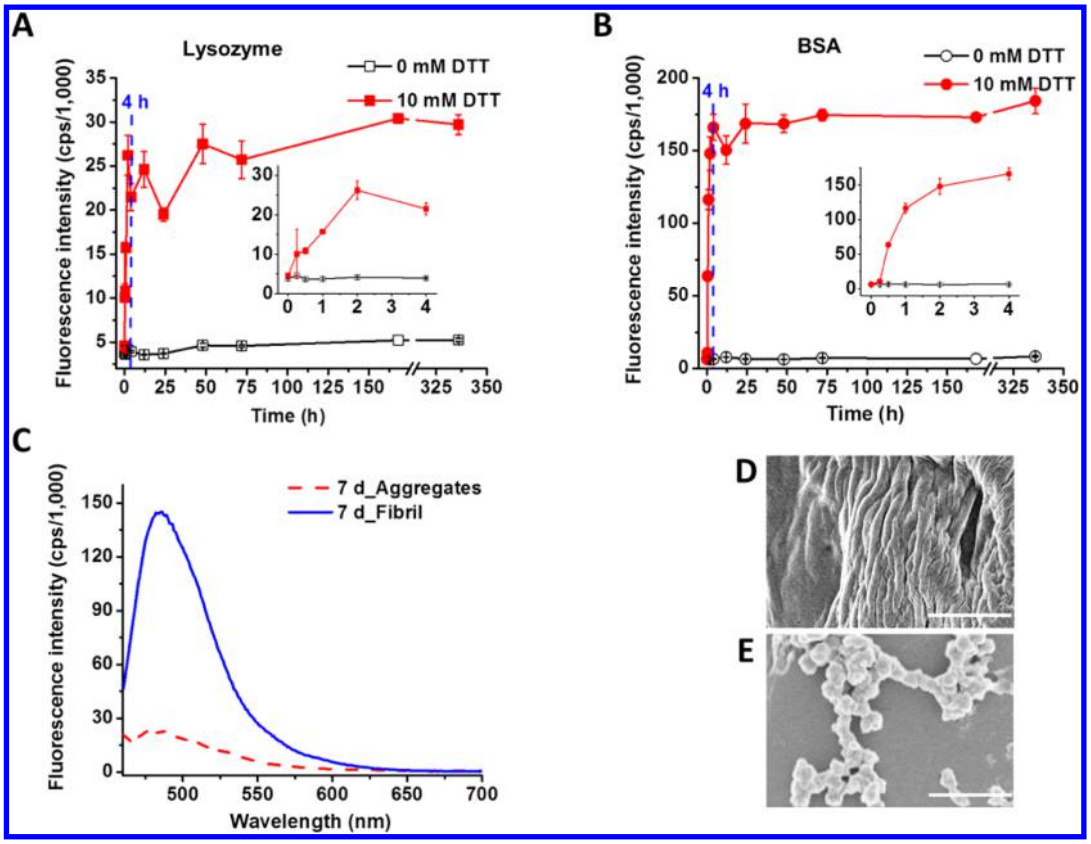

Figure 6. ThT fluorescence of protein aggregates and lysozyme fibrils. Emission spectra for 5 μM lysozyme and BSA in the presence of 10 μM ThT were acquired from 460 to 700 nm with excitation at 450 nm. Average emission peak wavelengths of 486 and 484 nm were selected for lysozyme (A) and BSA (B), respectively. Peak fluorescence intensities are shown as open symbols (without DTT) and closed symbols (with 10 mM DTT). The inset shows a plot for the first 4 h of incubation. Error bars indicate ± SD. (C) Fluorescence spectrum showing the signal for 5 μM lysozyme fibril and amorphous aggregates from 7-day-old samples incubated with 10 μM ThT dye. SEM images shows structures of lysozyme fibril (D) and lysozyme aggregates (E) from 7-day-old samples (scale bars = 5 μm).

fluorescence at ~485 nm.[48] Some of the studies exploring the molecular mechanism of ThT binding showed that the variance in fluorescence intensities of mature fibril and the aggregates could be due to difference in the binding modes of ThT on these structures or due to rotation of the single bond (φ) connecting the benzothiazole ring and the dimethylaminobenzene ring.[49−51] It is widely accepted that ThT binds to the grooves parallel to the long axis of amyloid fibrils and is stabilized by the hydrophobic and aromatic amino acid side-chains, leading to an increase in fluorescence.[49] Groenning and colleagues[50] showed that, if the binding site on the proteins was <8 Å, the ThT molecule could tightly bind without inducing the characteristic fluorescence as observed for β-sheet-rich proteins β-cyclodextrin and transthyretin. On the other hand, even non-β-sheet proteins such as γ-cyclodextrin and acetylcholinesterase, which have cavity diameters of 8−9 Å, could induce a high ThT fluorescence signal similar to that of amyloid fibrils.[50] Wolfe and colleagues[51] compared the monomeric and amyloid-like oligomer of β-2 microglobulin (β2m) crystallized with ThT and found that the angle φ of the ThT single bond is ~60° (twisted, excited state) in amyloid-like oligomers and is ~30° (close to planar, minimum energy conformation) for β2m monomers. In the current study, the DTT-treated aggregates show a distinct structure that is very different compared to amyloid fibrils (Figure 6D and E) but are very hydrophobic as indicated by ANS fluorescence (Figure 5A and B). Therefore, it is highly likely that ThT molecules could bind to the hydrophobic pockets of the aggregates, but due to the unique structure of aggregates (i.e., amorphous instead of fibril) can bind differently (close to planar orientation in amorphous; more twisted in fibril), resulting in weak fluorescence for amorphous and high fluorescence for fibril (Figure 6C). Even though the lysozyme aggregates in this study are more "structured", there is no direct evidence demonstrating that these aggregates could be classified as protofibrils or protofibril-like aggregates.

Nonreducing SDS-PAGE was used to visualize higher molecular weight cross-linked protein species that can arise due to the scrambling of disulfide bonds (Figure 3). The nonreducing gel electrophoresis for lysozyme shows the appearance of distinct high molecular weight bands as early as 4 h that can result from disulfide-bond scrambling (Figure 3A). This is in line with an earlier study that reported formation of scrambled disulfide bonds for lysozyme in the presence of 2-mercaptoethanol, a disulfide-reducing agent.[18] On the basis of an earlier study, the 17 disulfide bonds in BSA can be grouped in three classes centered on their location and susceptibility to disulfide-reducing agent: fully exposed (reactive with 0.5 mM DTT), partially buried (reactive with 10 mM DTT), and buried (nonreactive in native solution without any denaturants).[52] For a full reduction of disulfide bonds of the BSA polypeptide chain, 110−218-fold molar excess of DTT is required.[28] In this study, the use of 10 mM DTT is only a 14-fold molar excess for BSA disulfide bonds. Therefore, we do not expect complete

DOI: 10.1021/acs.jpcb.5b00144
J. Phys. Chem. B 2015, 119, 3969−3981

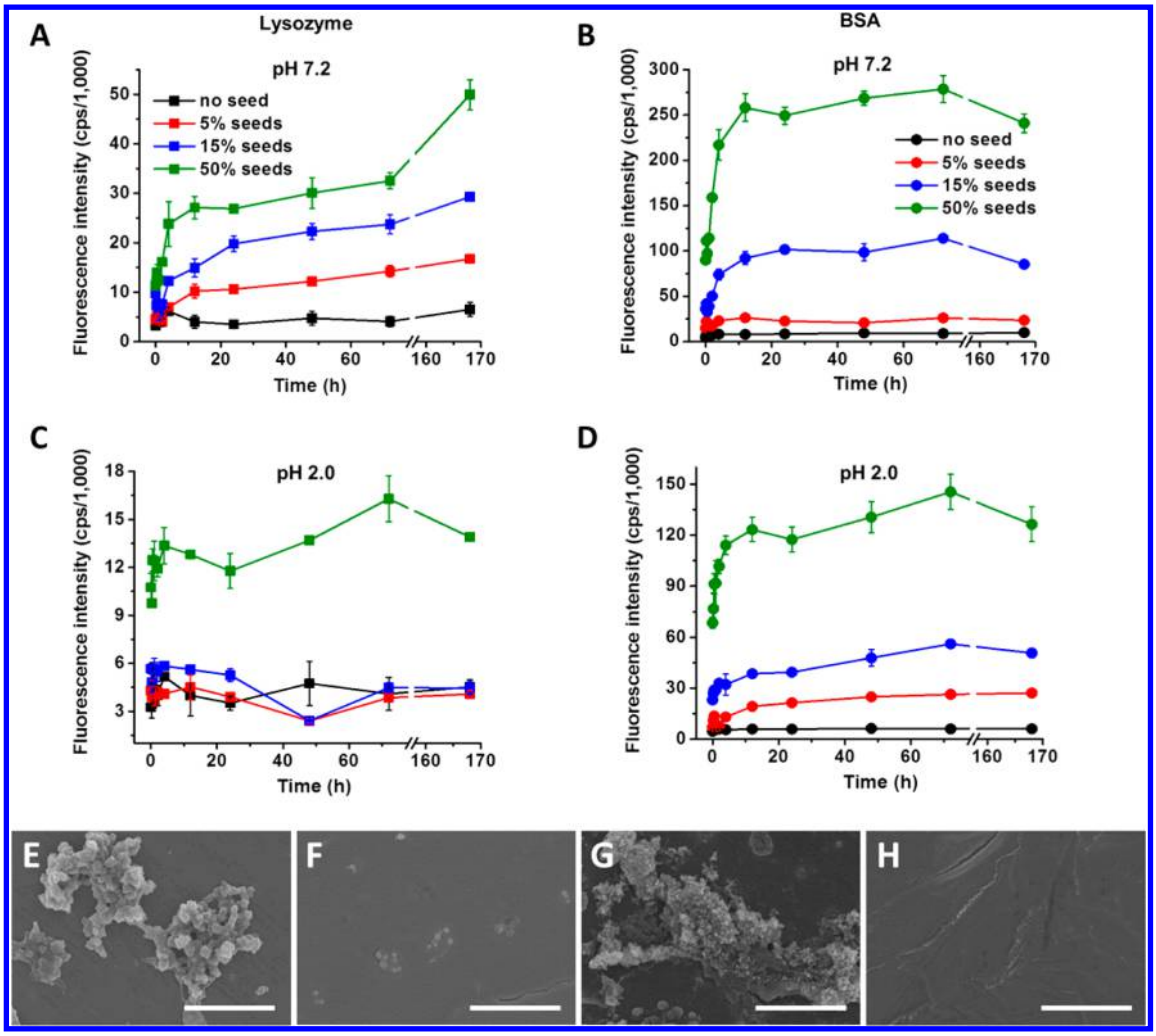

Figure 7. Effect of seeding of lysozyme and BSA aggregates on native protein monitored by ThT fluorescence. Five percent, 15%, and 50% (v/v) of aggregates generated by incubating lysozyme and BSA protein at pH 7.2 and in the presence of 10 mM DTT were added as seeds to 40 μM native protein solutions and incubated at 37 °C: lysozyme pH 7.2 (A and E), lysozyme pH 2.0 (C and F), BSA pH 7.2 (B and G), and BSA pH 2.0 (D and H). ThT fluorescence experiments were performed as detailed in Figure 6. Error bars indicate ± SD. SEM images (E–H) show the morphology of aggregates formed with 15% seeds after 72 h of incubation (scale bars = 10 μm).

reduction of all the disulfide bridges in the BSA polypeptide chain (Figure 3C; see lane R′). Partial disulfide reduction can promote scrambling of disulfide bonds, resulting in higher molecular weight species (Figure 3B). "R" and "O" bands indicate the presence of a mixture of reduced (R) and oxidized (O) proteins in the DTT-treated BSA samples after 4 h of incubation (Figure 3B). The presence of high molecular weight protein species in BSA samples treated with 40 or 100 mM DTT at 48 h suggests that proteins are not fully reduced even at high concentrations of DTT under the incubation conditions (Figure 3C). The atypical electrophoretic mobility of DTT-treated BSA samples is due to a mixture of partially oxidized and reduced proteins affecting the overall hydrodynamic volume of proteins (apparent size) and hence its migration on SDS-PAGE.[53,54] In the gel "R" and "O" bands started to be clearly visible from 2 h and their intensities did not change after 4 h which is in line with trend of fluorescence results (Figures 4B, 5B, and 6B). This suggests that the presence of scrambled (inter-/intramolecular) disulfide bonds may be critical in driving and further stabilizing the amorphous aggregate formation (Figures 2 and 9).

Intrinsic fluorescence can provide information on protein conformational changes by measuring tryptophan fluorescence that is very sensitive to its local microenvironment. Although both lysozyme and BSA showed similar aggregation kinetics with major structural changes observed within the first 4 h, they gave different fluorescence responses. Lysozyme showed an increase in intrinsic fluorescence for the first 4 h, followed by a rapid decrease in fluorescence signal (Figure 4A). The major contributors of intrinsic fluorescence in native lysozyme are Trp 62 and Trp 108,[55] which are exposed to the solvent.[56] The other Trp residues are either tightly packed inside the structure (Trp 111 and Trp 123) or are located near disulfide bonds (Trp 28, Trp 63, Trp 111, Trp 123), which have Cys-linked sulfurs that can act as fluorescence quenchers.[55] Therefore, the increase of lysozyme intrinsic fluorescence in the first 4 h could be a result of disulfide bonds breaking with and exposing Trp residues, decreasing the quenching effects of reduced sulfur groups in the unfolded structure. Free thiols upon longer incubation can form scrambled disulfide bonds and quench intrinsic fluorescence as the aggregated proteins may have a more packed structure that may also bring the Trp residues closer to Cys residues. DTT-treated BSA showed a very

DOI: 10.1021/acs.jpcb.5b00144
J. Phys. Chem. B 2015, 119, 3969–3981

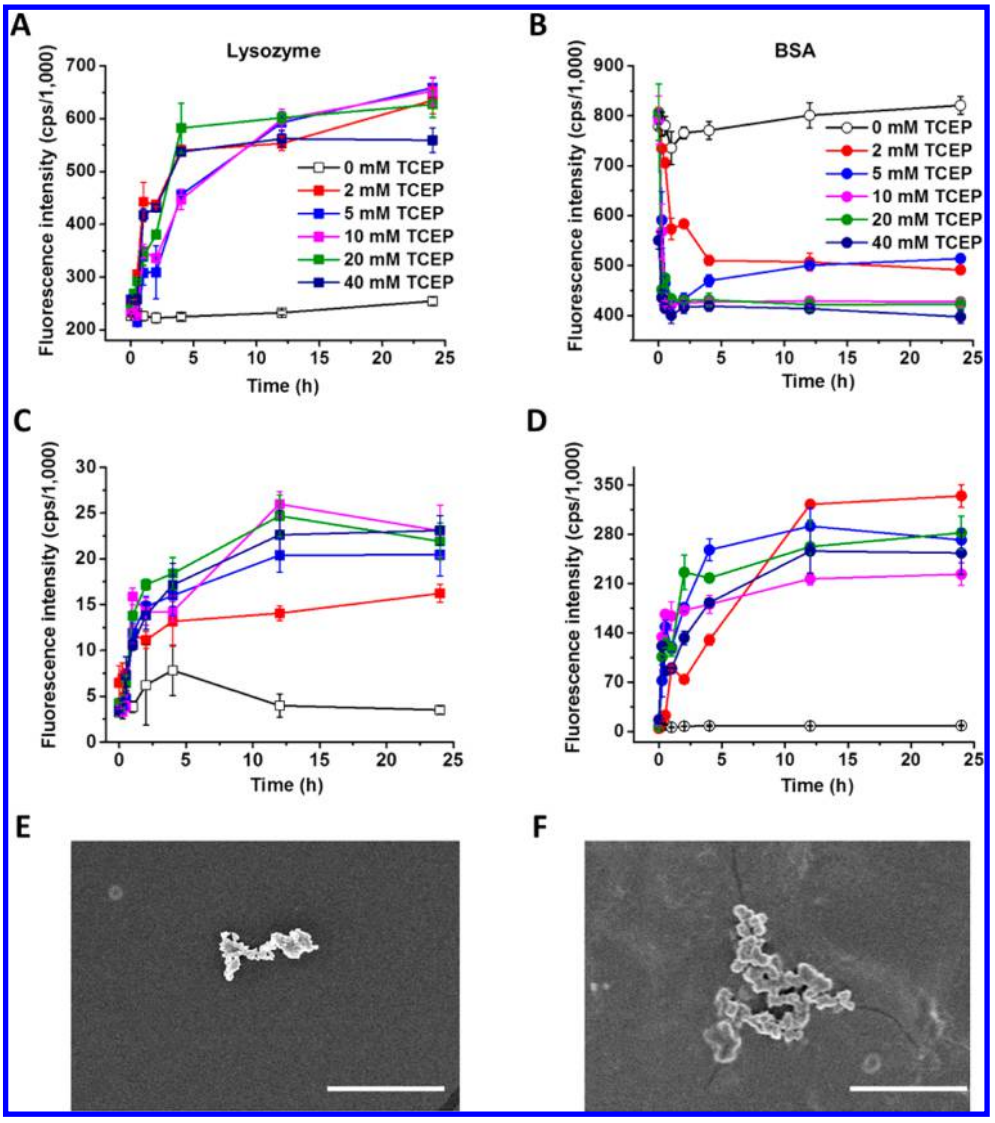

Figure 8. Concentration dependence of TCEP on protein aggregation. Protein aggregation rates were monitored using intrinsic fluorescence (A and B) and ThT fluorescence (C and D) for lysozyme (A and C) and BSA (B and D). Error bars indicate ± SD. Intrinsic fluorescence experiments were performed as detailed in Figure 4, and ThT fluorescence experiments were performed as detailed in Figure 6. SEM images for aggregates of lysozyme and BSA in the presence of 2 mM TCEP are shown in panels (E) and (F), respectively. Scale bars = 10 μm.

different fluorescence response than lysozyme (Figure 4B). The major difference may be due to the size of the protein (66 kDa), number of disulfide bonds (17 S−S bonds) per molecule of protein, and location of aromatic residues in the protein structure.[31] BSA is a big protein with only two tryptophan residues (W-134 and W-213), and neither of them is located on the protein's surface. A blue shift in the emission peak that is associated with a decrease in fluorescence intensity is consistent with aggregation leading to shielding of Trp residues and its fluorescence being quenched by close proximity of other groups such as free Cys or peptide bond[57,58] (Figure S13, Supporting Information).

As all of the Trp residues in lysozyme and BSA are located near hydrophobic clusters,[17,31,59] we used hydrophobic probe ANS to detect a change in protein hydrophobicity. ANS is very sensitive to local solvent environments, shows high fluorescence, and is blue-shifted when buried in hydrophobic pockets, or shows decreased fluorescence that is red-shifted when exposed to a more polar environment.[47,60,61] In the presence of ANS, lysozyme showed a rapid increase in fluorescence for the first 4 h with subsequent fluorescence plateau (Figure 5A). This was mirrored by a shift in wavelength for peak cps from ∼510 nm (considerable exposure to polar solvent) to ∼470 nm (indicative of buried in hydrophobic core) and was stable around 470 nm after that (Figure S14A, Supporting Information). The high fluorescence signal and blue shift suggests that lysozyme aggregates may be flexible, permitting tight binding of ANS molecules to the protein.[47,62,63] To further study the flexibility of protein aggregates, we used the dimeric analogue of ANS, bis-ANS, which has larger ring structure and does not bind tightly to organized structures, even if hydrophobic. Bis-ANS requires flexible molten globule-like structures for tight binding[64,65] and reacts weakly to amyloid fibrils.[66] Bis-ANS fluorescence of lysozyme aggregates suggests that DTT-reduced lysozyme aggregates have a highly flexible structure (Figure 5C). The continued high bis-ANS fluorescence of reduced lysozyme after 4 h indicates that aggregates of lysozyme even after long-term incubation were still flexible and had not converted into more organized and rigid structures. As ANS and bis-ANS have net negative charge,

DOI: 10.1021/acs.jpcb.5b00144
J. Phys. Chem. B 2015, 119, 3969−3981

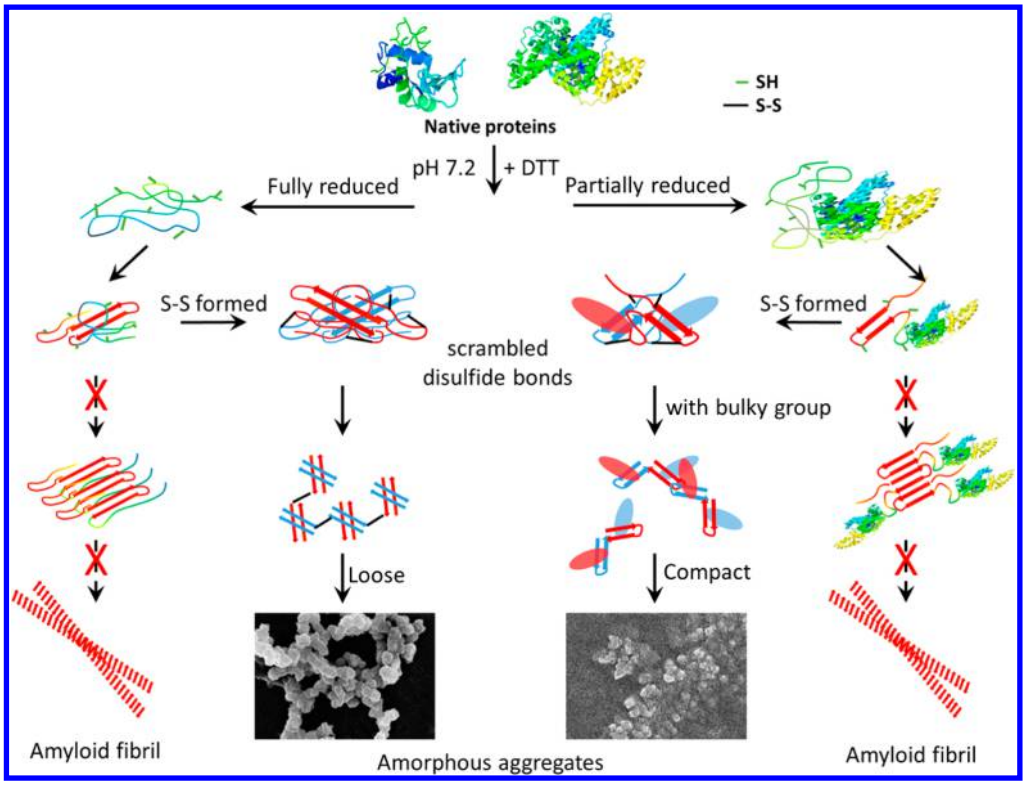

Figure 9. Generic aggregation model based on the results of both lysozyme and BSA proteins treated with 10 mM DTT at pH 7.2 and 37 °C. Incomplete reduction of disulfide bonds in proteins can affect misfolding and can result in the formation of scrambled disulfide bonds (both inter- and intramolecular), affecting the aggregation process. This can favor the formation of amorphous aggregates over the amyloid-like structure.

we investigated the effect of ionic strength on the fluorescence of lysozyme aggregates (Figure S15, Supporting Information). Although it has been reported that high ionic strength can affect lysozyme structure,[67] the removal of NaCl in this study did not affect lysozyme aggregation, suggesting that electrostatic interaction is not a major force driving of the interaction at pH 7.2.

Different from lysozyme, the reduced BSA showed a dramatic decrease in ANS fluorescence in the first 4 h and then was stable at low signal level for the long term (Figure 5B). The BSA samples with intact disulfide bonds (lacking DTT) showed high ANS fluorescence (Figure 5B). This could be because ANS can bind to the hydrophobic pockets on BSA and its fluorescence intensity and quantum yield depend upon the degree of exposure to solvent.[61,68] In addition, serum albumin is a transport protein with a highly flexible native structure and has many binding sites for lipids or drugs that can also bind ANS.[37] The decrease in ANS fluorescence of DTT-treated BSA could be due to exposure of the hydrophobic regions to the solvent phase, or collapsing and aggregating of hydrophobic regions that can be a result of scrambling of disulfide bonds, as BSA is only partially reduced under the experimental conditions. Peak emission wavelength for fluorescence in the 470 nm range suggests poor but hydrophobic binding of the dye, which may be a result of rigid amorphous structure (Figure S14B, Supporting Information). Bis-ANS was used to further investigate protein flexibility changes in oxidized and reduced BSA. Interestingly, we found that both DTT-treated and DTT-lacking BSA samples had weak interactions with bis-ANS and showed a decrease in fluorescence with time (Figure 5D). An earlier study by Celej and colleagues[65] shows that bis-ANS at low concentrations can bind to BSA, inducing tight conformers, and at high concentrations can induce disordered protein structures. Therefore, in the case of native BSA protein (not treated with DTT), the equilibrium could shift to a tighter conformer after binding bis-ANS. However, non-native conformation of BSA has only low-affinity bis-ANS binding sites.[65] The structures of DTT-treated BSA aggregates are relatively compact as indicated by intrinsic and ANS fluorescence (Figures 4B and 5B), suggesting weak binding with bis-ANS.

In the cross-seeding experiments, the amorphous aggregates were able to act as seeds and lead to rapid aggregation of native proteins at pH 7.2 (Figure 7), suggesting a low energy barrier between the native conformation and the aggregates.[69,70] In addition, the association of native proteins to seeds could also be driven by hydrophobic interactions, knowing that the aggregates have high ANS binding capacity (Figure 5), whereas the cross-seeded proteins at pH 2.0 (Figure 7) did not induce aggregation of native proteins. This may be due to the difference in molecular organization of native proteins that favor fibril formation at pH 2.0.[48] In addition, the scrambling of disulfide bonds increased the tendency for molecular self-assembling and collisions that result in the lack of large homogeneous structures. Similar findings have been reported in previous studies of amyloid-β peptide[48] and β2-microglobulin.[71] Therefore, the amorphous aggregates of disulfide-reduced proteins at pH 7.2 are probably formed through a kinetically trapped pathway, due to strong inter-/intramolecular association caused by disulfide scrambling.

To further confirm that the formation of amorphous aggregates observed in this study is a result of disulfide scrambling and not thiolated side product of DTT oxidation, we treated the proteins with 0–40 mM TCEP (Figure 8). It is

DOI: 10.1021/acs.jpcb.5b00144
J. Phys. Chem. B 2015, 119, 3969–3981

noticeable that, in the presence of 2 mM TCEP, both lysozyme and BSA show strong measurable fluorescence signals. Knowing that TCEP has a stronger reducing activity[72] and a longer half-life than DTT,[73] a high concentration of TCEP could inhibit disulfide scrambling, which is the driving force for the formation of amorphous aggregates observed in this study. SEM images of protein samples incubated with 2 mM TCEP formed amorphous aggregates (Figure 8 E and F) that share morphology very similar to 10 mM DTT-treated protein samples. However, we did not observe aggregates of either lysozyme or BSA up to 24 h with TCEP concentration higher than 5 mM. The high concentration of TCEP could possibly inhibit the scrambling of disulfide bonds and, hence, can affect the formation of amorphous aggregates. Because the result with 10 mM DTT could be reproduced with a low concentration of TCEP (2 mM), we believe that the formation of amorphous aggregates in the presence of 10 mM DTT is a result of disulfide scrambling.

CONCLUSIONS

In summary, under the experimental conditions reported in this work, both disulfide-reduced lysozyme and BSA showed increased susceptibility to form amorphous aggregates that have very distinct structures. Both proteins show increased ThT binding, but the fluorescence signal is still low compared to that for amyloid fibril. The lysozyme aggregates show higher structural flexibility in comparison to BSA aggregates. Formation of amorphous aggregates for these two proteins is a result of the interplay of disulfide bond scrambling and hydrophobic interactions that could kinetically affect the overall aggregation pathway (Figure 9). Cross-seeding experiments into native proteins for both proteins could only promote aggregation at pH 7.2, but not for proteins at acidic pH. This may be due to surface charge differences on proteins resulting in unique molecular organization at different pHs.

ASSOCIATED CONTENT

Supporting Information

Results of DTT concentration dependence test; TCEP concentration dependence study; SEM images of 14- and 48-day lysozyme aggregates, lysozyme fibrils, and aggregates formed by cross-seeding; Stokes shift of intrinsic and ANS fluorescence spectrum; nonreducing SDS-PAGE of insoluble fractions in samples; control trials of removing NaCl. This material is available free of charge via the Internet at http://pubs.acs.org.

AUTHOR INFORMATION

Corresponding Author

*Tel.: (906) 487-1840. Fax: (906) 487-2061. E-mail: tiwari@mtu.edu.

Author Contributions

A.T., M.Y., and C.D. designed the experiments. M.Y. and C.D. performed the experiments. A.T., M.Y., and C.D. analyzed the data. A.T. and M.Y. wrote the paper. All authors commented on the manuscript. All authors have given approval to the final version of the manuscript.

Notes

The authors declare no competing financial interest.

ACKNOWLEDGMENTS

We thank the anonymous reviewers for their insightful constructive criticisms that have made this paper much stronger and a better read. This work was supported by Michigan Technological University new faculty start-up funds and Research Excellence Fund to A.T.

REFERENCES

(1) Fink, A. L. Protein Aggregation: Folding Aggregates, Inclusion Bodies and Amyloid. *Folding Des.* **1998**, *3*, R9−R23.
(2) Ross, C. A.; Poirier, M. A. Protein Aggregation and Neurodegenerative Disease. *Nat. Med.* **2004**, *10*, S10−S17.
(3) Glabe, C. G. Structural Classification of Toxic Amyloid Oligomers. *J. Biol. Chem.* **2008**, *283*, 29639−29643.
(4) DeToma, A. S.; Salamekh, S.; Ramamoorthy, A.; Lim, M. H. Misfolded Proteins in Alzheimer's Disease and Type II Diabetes. *Chem. Soc. Rev.* **2012**, *41*, 608−621.
(5) Bernstein, S. L.; Dupuis, N. F.; Lazo, N. D.; Wyttenbach, T.; Condron, M. M.; Bitan, G.; Teplow, D. B.; Shea, J.; Ruotolo, B. T.; Robinson, C. V.; et al. Amyloid-Beta Protein Oligomerization and the Importance of Tetramers and Dodecamers in the Aetiology of Alzheimer's Disease. *Nat. Chem.* **2009**, *1*, 326−331.
(6) Krebs, M. R. H.; Wilkins, D. K.; Chung, E. W.; Pitkeathly, M. C.; Chamberlain, A. K.; Zurdo, J.; Robinson, C. V.; Dobson, C. M. Formation and Seeding of Amyloid Fibrils from Wild-Type Hen Lysozyme and a Peptide Fragment from the Beta-Domain. *J. Mol. Biol.* **2000**, *300*, 541−549.
(7) Morozova-Roche, L. A.; Zurdo, J.; Spencer, A.; Noppe, W.; Receveur, V.; Archer, D. B.; Joniau, M.; Dobson, C. M. Amyloid Fibril Formation and Seeding by Wild-Type Human Lysozyme and Its Disease-Related Mutational Variants. *J. Struct. Biol.* **2000**, *130*, 339−351.
(8) Bhattacharya, M.; Jain, N.; Mukhopadhyay, S. Insights into the Mechanism of Aggregation and Fibril Formation from Bovine Serum Albumin. *J. Phys. Chem. B* **2011**, *115*, 4195−4205.
(9) Cao, A. E.; Hu, D. Y.; Lai, L. H. Formation of Amyloid Fibrils from Fully Reduced Hen Egg White Lysozyme. *Protein Sci.* **2004**, *13*, 319−324.
(10) Qin, Z.; Hu, D.; Zhu, M.; Fink, A. L. Structural Characterization of the Partially Folded Intermediates of an Immunoglobulin Light Chain Leading to Amyloid Fibrillation and Amorphous Aggregation. *Biochemistry* **2007**, *46*, 3521−3531.
(11) Juarez, J.; Taboada, P.; Mosquera, V. Existence of Different Structural Intermediates on the Fibrillation Pathway of Human Serum Albumin. *Biophys. J.* **2009**, *96*, 2353−2370.
(12) Maeda, R.; Ado, K.; Takeda, N.; Taniguchi, Y. Promotion of Insulin Aggregation by Protein Disulfide Isomerase. *Biochim. Biophys. Acta, Proteins Proteomics* **2007**, *1774*, 1619−1627.
(13) Holm, N. K.; Jespersen, S. K.; Thomassen, L. V.; Wolff, T. Y.; Sehgal, P.; Thomsen, L. A.; Christiansen, G.; Andersen, C. B.; Knudsen, A. D.; Otzen, D. E. Aggregation and Fibrillation of Bovine Serum Albumin. *Biochim. Biophys. Acta, Proteins Proteomics* **2007**, *1774*, 1128−1138.
(14) Mossuto, M. F.; Dhulesia, A.; Devlin, G.; Frare, E.; Kumita, J. R.; de Laureto, P. P.; Dumoulin, M.; Fontana, A.; Dobson, C. M.; Salvatella, X. The Non-Core Regions of Human Lysozyme Amyloid Fibrils Influence Cytotoxicity. *J. Mol. Biol.* **2010**, *402*, 783−796.
(15) Dobson, C. M. Protein Folding and Misfolding. *Nature* **2003**, *426*, 884−890.
(16) Sarkar, N.; Kumar, M.; Dubey, V. K. Effect of Sodium Tetrathionate on Amyloid Fibril: Insight into the Role of Disulfide Bond in Amyloid Progression. *Biochimie* **2011**, *93*, 962−968.
(17) Silvers, R.; Sziegat, F.; Tachibana, H.; Segawa, S.; Whittaker, S.; Guenther, U. L.; Gabel, F.; Huang, J.; Blackledge, M.; Wirmer-Bartoschek, J.; et al. Modulation of Structure and Dynamics by Disulfide Bond Formation in Unfolded States. *J. Am. Chem. Soc.* **2012**, *134*, 6846−6854.

DOI: 10.1021/acs.jpcb.5b00144
J. Phys. Chem. B 2015, 119, 3969−3981

(18) Chang, J. Y.; Li, L. The Unfolding Mechanism and the Disulfide Structures of Denatured Lysozyme. *FEBS Lett.* **2002**, *511*, 73−78.
(19) Li, Y.; Yan, J.; Zhang, X.; Huang, K. Disulfide Bonds in Amyloidogenesis Diseases Related Proteins. *Proteins: Struct., Funct., Bioinf.* **2013**, *81*, 1862−1873.
(20) Li, Y.; Gong, H.; Sun, Y.; Yan, J.; Cheng, B.; Zhang, X.; Huang, J.; Yu, M.; Guo, Y.; Zheng, L.; Huang, K. Dissecting the Role of Disulfide Bonds on the Amyloid Formation of Insulin. *Biochem. Biophys. Res. Commun.* **2012**, *423*, 373−378.
(21) Wang, S. S. S.; Liu, K. N.; Wang, B. W. Effects of Dithiothreitol on the Amyloid Fibrillogenesis of Hen Egg-White Lysozyme. *Eur. Biophys. J.* **2010**, *39*, 1229−1242.
(22) Wu, G. Y.; Fang, Y. Z.; Yang, S.; Lupton, J. R.; Turner, N. D. Glutathione Metabolism and Its Implications for Health. *J. Nutr.* **2004**, *134*, 489−492.
(23) Wang, G. Z.; Dong, X. Y.; Sun, Y. The Role of Disulfide Bond Formation in the Conformational Folding Kinetics of Denatured/Reduced Lysozyme. *Biochem. Eng. J.* **2009**, *46*, 7−11.
(24) Michailidis, Y.; Karagounis, L. G.; Terzis, G.; Jamurtas, A. Z.; Spengos, K.; Tsoukas, D.; Chatzinikolaou, A.; Mandalidis, D.; Stefanetti, R. J.; Papassotiriou, I.; et al. Thiol-Based Antioxidant Supplementation Alters Human Skeletal Muscle Signaling and Attenuates Its Inflammatory Response and Recovery after Intense Eccentric Exercise. *Am. J. Clin. Nutr.* **2013**, *98*, 233−245.
(25) Sen, C. K. Redox Signaling and the Emerging Therapeutic Potential of Thiol Antioxidants. *Biochem. Pharmacol.* **1998**, *55*, 1747−1758.
(26) Rushworth, G. F.; Megson, I. L. Existing and Potential Therapeutic Uses for N-Acetylcysteine: The Need for Conversion to Intracellular Glutathione for Antioxidant Benefits. *Pharmacol. Ther.* **2014**, *141*, 150−159.
(27) Touch, V.; Hayakawa, S.; Saitoh, K. Relationships between Conformational Changes and Antimicrobial Activity of Lysozyme upon Reduction of Its Disulfide Bonds. *Food Chem.* **2004**, *84*, 421−428.
(28) Ueki, T.; Hiragi, Y.; Kataoka, M.; Inoko, Y.; Amemiya, Y.; Izumi, Y.; Tagawa, H.; Muroga, Y. Aggregation of Bovine Serum Albumin upon Cleavage of Its Disulfide Bonds, Studied by the Time-Resolved Small-Angle X-ray Scattering Technique with Synchrotron Radiation. *Biophys. Chem.* **1985**, *23*, 115−124.
(29) Tiwari, A.; Hayward, L. J. Familial Amyotrophic Lateral Sclerosis Mutants of Copper/Zinc Superoxide Dismutase Are Susceptible to Disulfide Reduction. *J. Biol. Chem.* **2003**, *278*, 5984−5992.
(30) Nagendra, H. G.; Sudarsanakumar, C.; Vijayan, M. An X-ray Analysis of Native Monoclinic Lysozyme. A Case Study on the Reliability of Refined Protein Structures and a Comparison with the Low-Humidity Form in Relation to Mobility and Enzyme Action. *Acta Crystallogr., Sect. D: Biol. Crystallogr.* **1996**, *52*, 1067−1074.
(31) Bujacz, A. Structures of Bovine, Equine and Leporine Serum Albumin. *Acta Crystallogr., Sect. D: Biol. Crystallogr.* **2012**, *68*, 1278−1289.
(32) Guez, V.; Roux, P.; Navon, A.; Goldberg, M. E. Role of Individual Disulfide Bonds in Hen Lysozyme Early Folding Steps. *Protein Sci.* **2002**, *11*, 1136−1151.
(33) White, F. H. Studies on the Relationship of Disulfide Bonds to the Formation and Maintenance of Secondary Structure in Chicken Egg-White Lysozyme. *Biochemistry* **1982**, *21*, 967−977.
(34) Vernaglia, B. A.; Huang, J.; Clark, E. D. Guanidine Hydrochloride Can Induce Amyloid Fibril Formation from Hen Egg-White Lysozyme. *Biomacromolecules* **2004**, *5*, 1362−1370.
(35) Raccosta, S.; Manno, M.; Bulone, D.; Giacomazza, D.; Militello, V.; Martorana, V.; San Biagio, P. L. Irreversible Gelation of Thermally Unfolded Proteins: Structural and Mechanical Properties of Lysozyme Aggregates. *Eur. Biophys. J.* **2010**, *39*, 1007−1017.
(36) Navarra, G.; Troia, F.; Militello, V.; Leone, M. Characterization of the Nucleation Process of Lysozyme at Physiological pH: Primary but Not Sole Process. *Biophys. Chem.* **2013**, *177*, 24−33.
(37) He, X. M.; Carter, D. C. Atomic Structure and Chemistry of Human Serum Albumin. *Nature* **1992**, *358*, 209−215.
(38) Katchalski, E.; Benjamin, G. S.; Gross, V. The Availability of the Disulfide Bonds of Human and Bovine Serum Albumin and of Bovine Gamma-Globulin to Reduction by Thioglycolic Acid. *J. Am. Chem. Soc.* **1957**, *79*, 4096−4099.
(39) Borzova, V. A.; Markossian, K. A.; Kurganov, B. I. Relationship between the Initial Rate of Protein Aggregation and the Lag Period for Amorphous Aggregation. *Int. J. Biol. Macromol.* **2014**, *68*, 144−150.
(40) Davidson, B. E.; Hird, F. J. The Reactivity of the Disulphide Bonds of Purified Proteins in Relationship to Primary Structure. *Biochem. J.* **1967**, *104*, 473−9.
(41) Johanson, K. O.; Wetlaufer, D. B.; Reed, R. G.; Peters, T. Refolding of Bovine Serum-Albumin and Its Proteolytic Fragments. Regain of Disulfide Bonds, Secondary Structure, and Ligand-Binding Ability. *J. Biol. Chem.* **1981**, *256*, 445−450.
(42) Vetri, V.; D'Amico, M.; Fodera, V.; Leone, M.; Ponzoni, A.; Sberveglieri, G.; Militello, V. Bovine Serum Albumin Protofibril-Like Aggregates Formation: Solo but Not Simple Mechanism. *Arch. Biochem. Biophys.* **2011**, *508*, 13−24.
(43) Arasteh, A.; Habibi-Rezaei, M.; Ebrahim-Habibi, A.; Moosavi-Movahedi, A. A. Response Surface Methodology for Optimizing the Bovine Serum Albumin Fibrillation. *Protein J.* **2012**, *31*, 457−465.
(44) Kumar, S.; Ravi, V. K.; Swaminathan, R. How Do Surfactants and DTT Affect the Size, Dynamics, Activity and Growth of Soluble Lysozyme Aggregates? *Biochem. J.* **2008**, *415*, 275−288.
(45) Mossuto, M. E.; Bolognesi, B.; Guixer, B.; Dhulesia, A.; Agostini, F.; Kumita, J. R.; Tartaglia, G. G.; Dumoulin, M.; Dobson, C. M.; Salvatella, X. Disulfide Bonds Reduce the Toxicity of the Amyloid Fibrils Formed by an Extracellular Protein. *Angew. Chem., Int. Ed.* **2011**, *50*, 7048−7051.
(46) Bucciantini, M.; Giannoni, E.; Chiti, F.; Baroni, F.; Formigli, L.; Zurdo, J. S.; Taddei, N.; Ramponi, G.; Dobson, C. M.; Stefani, M. Inherent Toxicity of Aggregates Implies a Common Mechanism for Protein Misfolding Diseases. *Nature* **2002**, *416*, 507−511.
(47) Hawe, A.; Sutter, M.; Jiskoot, W. Extrinsic Fluorescent Dyes as Tools for Protein Characterization. *Pharm. Res.* **2008**, *25*, 1487−1499.
(48) Yamaguchi, T.; Yagi, H.; Goto, Y.; Matsuzaki, K.; Hoshino, M. A Disulfide-Linked Amyloid-Beta Peptide Dimer Forms a Protofibril-Like Oligomer through a Distinct Pathway from Amyloid Fibril Formation. *Biochemistry* **2010**, *49*, 7100−7107.
(49) Biancalana, M.; Koide, S. Molecular Mechanism of Thioflavin-T Binding to Amyloid Fibrils. *Biochim. Biophys. Acta* **2010**, *1804*, 1405−1412.
(50) Groenning, M.; Olsen, L.; van de Weert, M.; Flink, J. M.; Frokjaer, S.; Jorgensen, F. S. Study on the Binding of Thioflavin T to Beta-Sheet-Rich and Non-Beta-Sheet Cavities. *J. Struct. Biol.* **2007**, *158*, 358−369.
(51) Wolfe, L. S.; Calabrese, M. F.; Nath, A.; Blaho, D. V.; Miranker, A. D.; Xiong, Y. Protein-Induced Photophysical Changes to the Amyloid Indicator Dye Thioflavin T. *Proc. Natl. Acad. Sci. U. S. A.* **2010**, *107*, 16863−16868.
(52) Malhotra, M.; Sahal, D. Anomalous Mobility of Sulfitolysed Proteins in SDS-PAGE—Analysis and Applications. *Int. J. Pept. Protein Res.* **1996**, *48*, 240−248.
(53) Tiwari, A.; Liba, A.; Sohn, S. H.; Seetharaman, S. V.; Bilsel, O.; Matthews, C. R.; Hart, P. J.; Valentine, J. S.; Hayward, L. J. Metal Deficiency Increases Aberrant Hydrophobicity of Mutant Superoxide Dismutases That Cause Amyotrophic Lateral Sclerosis. *J. Biol. Chem.* **2009**, *284*, 27746−27758.
(54) Sondack, D. L. Albert Light. Comparative Studies on the Modification of Specific Disulfide Bonds of Trypsinogen and Chymotrypsinogen. *J. Biol. Chem.* **1971**, *246*, 1630−1637.
(55) Laurents, D. V.; Baldwin, R. L. Characterization of the Unfolding Pathway of Hen Egg White Lysozyme. *Biochemistry* **1997**, *36*, 1496−1504.
(56) Baldwin, R. L. Protein Folding—Making a Network of Hydrophobic Clusters. *Science* **2002**, *295*, 1657−1658.
(57) Babcock, J. J.; Brancaleon, L. Bovine Serum Albumin Oligomers in the E- and B-Forms at Low Protein Concentration and Ionic Strength. *Int. J. Biol. Macromol.* **2013**, *53*, 42−53.

DOI: 10.1021/acs.jpcb.5b00144
J. Phys. Chem. B 2015, 119, 3969−3981

(58) Adams, P. D.; Chen, Y.; Ma, K.; Zagorski, M. G.; Sonnichsen, F. D.; McLaughlin, M. L.; Barkley, M. D. Intramolecular Quenching of Tryptophan Fluorescence by the Peptide Bond in Cyclic Hexapeptides. *J. Am. Chem. Soc.* **2002**, *124*, 9278−9286.
(59) Klein-Seetharaman, J.; Oikawa, M.; Grimshaw, S. B.; Wirmer, J.; Duchardt, E.; Ueda, T.; Imoto, T.; Smith, L. J.; Dobson, C. M.; Schwalbe, H. Long-Range Interactions within a Nonnative Protein. *Science* **2002**, *295*, 1719−1722.
(60) Lindgren, M.; Sorgjerd, K.; Hammarstrom, P. Detection and Characterization of Aggregates, Prefibrillar Amyloidogenic Oligomers, and Protofibrils Using Fluorescence Spectroscopy. *Biophys. J.* **2005**, *88*, 4200−4212.
(61) Matulis, D.; Baumann, C. G.; Bloomfield, V. A.; Lovrien, R. E. 1-Anilino-8-Naphthalene Sulfonate as a Protein Conformational Tightening Agent. *Biopolymers* **1999**, *49*, 451−458.
(62) Cunningham, E. L.; Agard, D. A. Interdependent Folding of the N- and C-Terminal Domains Defines the Cooperative Folding of Alpha-Lytic Protease. *Biochemistry* **2003**, *42*, 13212−13219.
(63) Semisotnov, G. V.; Rodionova, N. A.; Razgulyaev, O. I.; Uversky, V. N.; Gripas, A. F.; Gilmanshin, R. I. Study of the Molten Globule Intermediate State in Protein Folding by a Hydrophobic Fluorescent-Probe. *Biopolymers* **1991**, *31*, 119−128.
(64) Shi, L.; Palleros, D. R.; Fink, A. L. Protein Conformational-Changes Induced by 1,1′-Bis(4-Anilino-5-Naphthalenesulfonic Acid): Preferential Binding to the Molten Globule of DnaK. *Biochemistry* **1994**, *33*, 7536−7546.
(65) Celej, M. S.; Montich, C. G.; Fidelio, G. D. Protein Stability Induced by Ligand Binding Correlates with Changes in Protein Flexibility. *Protein Sci.* **2003**, *12*, 1496−1506.
(66) LeVine, H. 4,4′-Dianilino-1,1′-Binaphthyl-5,5′-Disulfonite: Report on Non-Beta-Sheet Conformers of Alzheimer's Peptide Beta(1−40). *Arch. Biochem. Biophys.* **2002**, *404*, 106−115.
(67) Takekiyo, T.; Yamazaki, K.; Yamaguchi, E.; Abe, H.; Yoshimura, Y. High Ionic Liquid Concentration-Induced Structural Change of Protein in Aqueous Solution: A Case Study of Lysozyme. *J. Phys. Chem. B* **2012**, *116*, 11092−11097.
(68) Togashi, D. M.; Ryder, A. G. Time-Resolved Fluorescence Studies on Bovine Serum Albumin Denaturation Process. *J. Fluoresc.* **2006**, *16*, 153−160.
(69) Dobson, C. M. Principles of Protein Folding, Misfolding and Aggregation. *Semin. Cell Dev. Biol.* **2004**, *15*, 3−16.
(70) Sanchez-Ruiz, J. M. Protein Kinetic Stability. *Biophys. Chem.* **2010**, *148*, 1−15.
(71) Hong, D. P.; Gozu, M.; Hasegawa, K.; Naiki, H.; Goto, Y. Conformation of Beta(2)-Microglobulin Amyloid Fibrils Analyzed by Reduction of the Disulfide Bond. *J. Biol. Chem.* **2002**, *277*, 21554−21560.
(72) Han, J. C.; Han, G. Y. A Procedure for Quantitative-Determination of Tris(2-Carboxyethyl)Phosphine, an Odorless Reducing Agent More Stable and Effective Than Dithiothreitol. *Anal. Biochem.* **1994**, *220*, 5−10.
(73) Getz, E. B.; Xiao, M.; Chakrabarty, T.; Cooke, R.; Selvin, P. R. A Comparison between the Sulfhydryl Reductants Tris(2-Carboxyethyl)-Phosphine and Dithiothreitol for Use in Protein Biochemistry. *Anal. Biochem.* **1999**, *273*, 73−80.

DOI: 10.1021/acs.jpcb.5b00144
J. Phys. Chem. B 2015, 119, 3969−3981